El Cezeri
Journal of Science and Engineering
ISSN: 2148-3736

Research Article

A Compact Coupled-Line Butterworth Bandpass Filter for Sub-6 GHz Applications

Burak Acikalin[1a], Nursel Akcam[2b], and Burak Dokmetas[3c]
[1]Department of Electrical and Electronics Engineering, Turkish Aeronautical Association University, Ankara,Türkiye
[2]Department of Electrical and Electronics Engineering, Gazi University, Ankara, 06570, Türkiye
[3]Department of Electrical and Electronics Engineering, Kafkas University, Kars, 36100, Türkiye

burakd@kafkas.edu.tr

DOI : 10.31202/ecjse.1842913
Received: 15.12.2025 Accepted: 16.03.2026
How to cite this article:
Acikalin B., Akcam N., and Dokmetas B., "A Compact Coupled-Line Butterworth Bandpass Filter for Sub-6 GHz Applications", El-Cezeri Journal of Science and Engineering, Vol: 13, Iss: 3, (2026), pp.(409-416).
ORCID: [a]0000-0002-7800-0073, [b]0000-0003-0585-3988, [c]0000-0001-5900-6691.

Abstract This paper presents the design, fabrication, and experimental validation of a compact microstrip bandpass filter operating at 3.5 GHz for sub-6 GHz 5G wireless communication systems. The proposed filter is realized using a fourth-order Butterworth response implemented through a parallel coupled-line topology, aiming to achieve a maximally flat passband response, low insertion loss, and sufficient selectivity within the n77 frequency band (3.3-3.8 GHz). The design procedure starts with the synthesis of a normalized low-pass Butterworth prototype, followed by bandpass transformation and its implementation as an equivalent distributed microstrip structure. Electromagnetic analysis and parametric optimization are employed to accurately model coupling effects, transmission line behavior, and fabrication constraints. The filter is fabricated on a low-cost FR-4 substrate with a dielectric constant of 4.3 and a thickness of 0.8 mm using standard printed circuit board manufacturing techniques. Experimental characterization is performed using a vector network analyzer to evaluate the frequency response. Measurement results demonstrate a center frequency of 3.5 GHz with an impedance bandwidth of approximately 300 MHz, showing good agreement with the predicted performance. The proposed bandpass filter offers a compact footprint, simple geometry, and reliable frequency response, making it a suitable candidate for integration into 5G radio-frequency front-end modules and other modern wireless communication systems.

Keywords: Butterworth response, Coupled-line topology, Microstrip bandpass filter, Sub-6 GHz 5G systems

1. INTRODUCTION

The rapid evolution of wireless communication technologies has led to an increasing demand for compact, high-performance, and low-loss microwave components suitable for modern broadband systems. In this context, microstrip bandpass filters constitute one of the most essential building blocks in radio-frequency (RF) front-end architectures, as they enable signal transmission within the desired frequency band while performing critical functions such as channel selection, harmonic suppression, and noise reduction in transmitter-receiver chains [1]. With the continuous growth in bandwidth requirements and data rates, the development of efficient filter structures capable of operating at higher frequencies with minimal insertion loss has become a key research focus.

The 3.5 GHz frequency band has emerged as a particularly attractive spectrum for fifth-generation (5G) mobile communication systems. Within this range, the n77 band (3.3-3.8 GHz) has been widely adopted due to its favorable balance between coverage and capacity, making it well suited for sub-6 GHz 5G deployments [2]. Nevertheless, filter design in this band remains challenging, as it requires the simultaneous fulfillment of stringent performance criteria, including low insertion loss, adequate out-of-band suppression, and compatibility with compact and densely integrated RF modules.

Microstrip filter technologies are extensively employed in wireless systems owing to their planar structure, ease of fabrication, and compatibility with standard printed circuit board processes, which together offer a reliable and cost-effective solution. Over the past years, various microstrip filter and microstrip antenna topologies-such as interdigital, hairpin, coupled-line, and step-impedance configurations-have been investigated and compared in the literature [3]-[8]. Recent studies have also demonstrated the versatility of planar and resonant RF structures for wireless applications through ANN-assisted microstrip antenna optimization, compact microstrip antennas for healthcare monitoring, and high-efficiency rectenna configurations based on dielectric resonant antennas [9]-[11]. Each of these approaches provides specific advantages in terms of size reduction, selectivity, stopband performance, and bandwidth. For instance, coupled-line filters are known for their structural simplicity and predictable performance, whereas interdigital and step-impedance designs can achieve compact

layouts and improved noise suppression characteristics [12], [13]. Despite these advancements, achieving an optimal trade-off between compactness, selectivity, and insertion loss continues to be an open design challenge.

To overcome the limitations of conventional filter structures, recent studies have increasingly focused on Butterworth-based filter responses, which are well known for providing a maximally flat passband characteristic and preserving signal integrity in wideband communication systems [14]. The incorporation of Butterworth responses into microstrip filter designs has shown promise in improving passband flatness; however, maintaining compact size and sufficient selectivity simultaneously remains nontrivial. In this regard, the integration of Butterworth characteristics with alternative resonator configurations, such as interdigital or step-impedance sections, has been explored to enhance suppression bandwidth control and overall filter performance [15], [16].

In terms of novelty, this study distinguishes itself from existing microstrip bandpass filter designs through the combined use of a fourth-order Butterworth response and a folded parallel coupled-line topology specifically tailored for sub-6 GHz 5G applications. Unlike conventional straight coupled-line or hairpin-based Butterworth filters, the proposed folded configuration enables a noticeable size reduction while preserving a maximally flat passband response and low insertion loss. Furthermore, the filter is fully realized on a low-cost FR-4 substrate and experimentally validated, demonstrating that high selectivity and compactness can be simultaneously achieved without relying on expensive or multilayer technologies. These features collectively highlight the originality of the proposed design and its practical relevance for compact 5G RF front-end modules.

2. DESIGN AND ANALYSIS OF THE PROPOSED BANDPASS FILTER

The proposed filter is designed to operate at a center frequency of 3.5 GHz with an impedance bandwidth of approximately 300 MHz, covering the frequency range from 3.35 GHz to 3.65 GHz within the n77 band allocated for 5G communication systems. This frequency band has gained significant importance in next-generation wireless networks due to its favorable characteristics in terms of transmission capacity and spectral efficiency [17].

The design procedure begins with the selection of an appropriate filter prototype. A Butterworth response is adopted owing to its maximally flat amplitude characteristic in the passband and inherent stability. FR-4 is chosen as the substrate material because of its wide availability, low cost, and stable electrical properties within the operating frequency range considered in this study [18]. The substrate thickness is set to 0.8 mm, while the copper metallization thickness is selected as 0.035 mm. The filter order is determined as four in order to satisfy the target performance criteria, namely a return loss (S_{11}) below -30 dB and an insertion loss (S_{21}) better than -3 dB within the passband.

Following the determination of the filter order, the lumped element values of the normalized low-pass Butterworth prototype are calculated and subsequently denormalized according to the specified center frequency and bandwidth requirements [19]. Based on these values, a fourth-order low-pass prototype circuit is obtained. The input and output ports are terminated with a characteristic impedance of 50 Ω. In order to realize the desired bandpass response, the low-pass prototype is transformed into its bandpass equivalent using standard frequency transformation techniques, as described in [20].

The fractional bandwidth is defined as equation (1);

$$\Delta = \frac{w_2 - w_1}{w_0} \tag{1}$$

where *w1* and *w2* denote the lower and upper cutoff angular frequencies, respectively, and *w0* represents the center angular frequency. For the bandpass transformation, each series inductance in the low-pass prototype is replaced by a series resonant circuit composed of an inductance *Ls* and a capacitance *Cs* while each shunt capacitance is replaced by a parallel resonant circuit composed of an inductance *Lp* and a capacitance *Cp*. The corresponding element values are obtained using the following standard relations (2) and (3):

$$L_S = \frac{L}{w_0 \Delta} \qquad C_S = \frac{\Delta}{w_0 L} \tag{2}$$

$$L_p = \frac{\Delta}{w_0 C} \qquad C_P = \frac{C}{w_0 \Delta} \tag{3}$$

These transformations preserve the frequency response characteristics of the original Butterworth prototype while shifting the response from the low-pass domain to the desired bandpass region. The resulting lumped-element bandpass circuit serves as the basis for subsequent conversion into an equivalent distributed microstrip structure.

After the lumped element values of the bandpass prototype are obtained, the circuit is transformed into an equivalent distributed microstrip configuration suitable for practical implementation. This transformation enables the realization of the lumped inductive and capacitive elements using microstrip transmission line sections with appropriate electrical lengths and characteristic impedances, as commonly adopted in planar filter design methodologies [20]. In this approach, the frequency-dependent behavior of inductors and capacitors is emulated through open- and short-circuited transmission line segments, allowing the bandpass response to be preserved in a physically realizable structure.

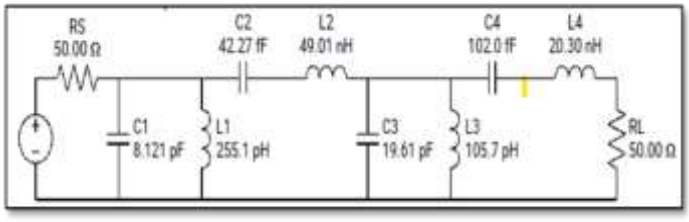


Figure 1. Lumped-Element Butterworth Bandpass Filter Prototype

The proposed filter topology is developed based on a parallel coupled-line configuration, which is widely used due to its structural simplicity and predictable coupling characteristics. In order to improve compactness and enhance overall performance, each coupled-line section is geometrically modified by introducing bends at specific intervals, forming paired coupled segments whose effective electrical length is reduced compared to a conventional straight coupled-line arrangement. This folded configuration enables a significant reduction in the overall footprint of the filter while maintaining the required coupling strength and passband characteristics.

The dimensions of the microstrip transmission lines are calculated using standard closed-form expressions that relate the characteristic impedance and effective dielectric constant to the physical width and height of the substrate. In these calculations, the characteristic impedance is selected as $Z0$ =50, the substrate height is set to h=0.8 mm, the relative dielectric constant is taken as εr =4.3, and the initial microstrip line width is chosen as W=1.5 mm. These parameters serve as the basis for determining the electrical lengths and coupling gaps of the microstrip sections used in the distributed filter structure.

For $\left(\frac{w}{h} < 2\right)$;

$$A = \frac{Z_c}{60} \times \sqrt{\frac{(e_r+1)}{2}} + \frac{(e_r-1)}{(e_r+1)} \times \left(0.23 + \frac{0.11}{e_r}\right) \tag{4}$$

For $\left(\frac{w}{h} > 2\right)$;

$$B = 377 \times \frac{\pi}{2 \times Z_0 \times \sqrt{e_r}} \tag{5}$$

$$\frac{w}{h} = \frac{2}{\pi} \times \left(B - 1 - \ln(2 \times B - 1) + \left(\frac{e_r - 1}{2e_r}\right) \times \left(\ln(B-1) + 0.39 - \frac{0.61}{e_r}\right)\right) \tag{6}$$

In parallel coupling design, the impedance calculation for both the even and odd mode is performed as described below for each degree.

$$Z_0 J_1 = \sqrt{\frac{\pi}{2g_1}} \frac{\Delta w}{w_0} \tag{7}$$

$$Z_0 J_n = \frac{\pi}{2\sqrt{g_{n-1} g_n}} \frac{\Delta w}{w_0} \tag{8}$$

$$Z_0 J_{N+1} = \sqrt{\frac{\pi}{2g_N g_{N+1}}} \frac{\Delta w}{w_0} \tag{9}$$

The impedances for coupled lines have been optimized to meet the coupling coefficient for operation within the desired frequency range for both dual and single modes. The calculated values for each mode are available in Table 1.

Table 1: Even and Odd Mode Impedances

Coupling Step	Admittance Inverter	Even Mode Impedance (Z_e)	Odd Mode Impedance (Z_0)
1	0.4192	79.74	37.82
2	0.1131	56.30	44.98
3	0.072	53.85	46.65
4	0.1131	56.30	44.98
5	0.4192	79.74	37.82

Based on these data, dimensional calculations for the circuit design were performed both manually and using the ADS program, and the results were observed after optimization. The three-dimensional design was obtained in the CST Microwave Studio program, where full-wave 3D electromagnetic simulations were performed, as shown in Figure 2.

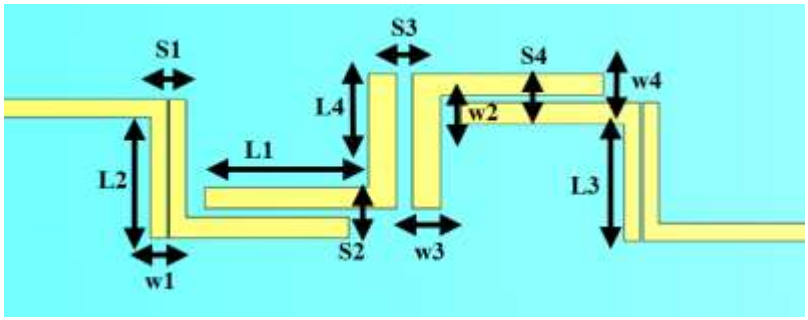


Figure 2. Layout of the proposed folded coupled-line microstrip Bandpass Filter

The entire filter structure, coupling gaps, resonator lengths, and feed line positions and dimensions have been parametrically optimized in the CST program to ensure the most accurate measurements. The coupling gaps between resonators, which significantly affect bandwidth and insertion loss, have been carefully calculated. The input/output feed lines have been tapered to reduce loss between the filter network and the 50 ohm SMA connector. The initial dimensions obtained from analytical calculations and the final optimized values resulting from electromagnetic optimization are presented in Table 2**.**

Table 2: Optimized Dimensional Values

Line Description	Calculated Filter Dimensions			Optimized Filter Sizes		
	W (mm)	S (mm)	L (mm)	W (mm)	S (mm)	L (mm)
Coupling Line 1	W1=1.17	S1=0.16	L1=12	W1=1	S1=0.12	L1=12.3
Coupling Line 2	W2=1.85	S2=0.8	L2=11.7	W2=1.55	S2=0.88	L2=11.6
Coupling Line 3	W3=2	S3=1.18	L3=11.7	W3=1.8	S3=1.55	L3=11.6
Coupling Line 4	W4=1.85	S4=0.8	L4=11.7	W4=1.55	S4=0.88	L4=11.6

After validating the simulated results, the proposed filter was realized using conventional printed circuit board (PCB) fabrication methods. The designed layout was implemented on an FR-4 substrate employing a standard photolithographic etching procedure. For experimental evaluation, SMA connectors were carefully mounted at the input and output interfaces of the fabricated prototype. The front-side view of the manufactured microstrip bandpass filter is depicted in Figure 3, whereas the rear-side configuration of the structure is shown in Figure 4.

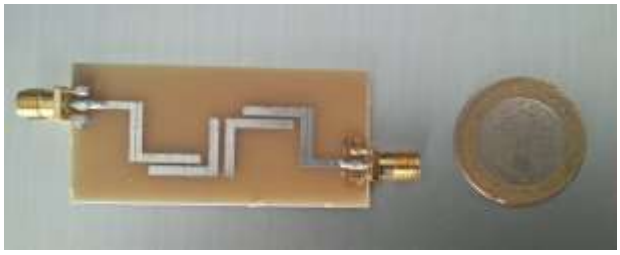


Figure 3. Top view of the fabricated microstrip Bandpass Filter prototype

The fabricated filter occupies an overall area of 60 × 30 mm, which corresponds to approximately $0.70\lambda_o \times 0.35\lambda_o$ at the operating frequency of 3.5 GHz. The proposed design methodology covering theoretical formulation, circuit transformation, and experimental realization demonstrates that the filter fulfills the requirements of sub-6 GHz 5G systems by achieving a compact layout, low insertion loss, and sufficient suppression in the out-of-band regions.



Figure 4. Bottom view of the fabricated microstrip Bandpass Filter prototype

3. SIMULATION AND EXPERIMENTAL RESULTS

The designed bandpass filter was analyzed using full-wave electromagnetic simulations to evaluate its frequency response and scattering parameters. The simulated magnitude responses of the reflection coefficient (S_{11}) and transmission coefficient (S_{21}) are presented in Figure 5, illustrating the filter behavior in both the passband and stopband regions. The results clearly demonstrate the intended bandpass characteristics around the center frequency, along with adequate attenuation outside the operating band.

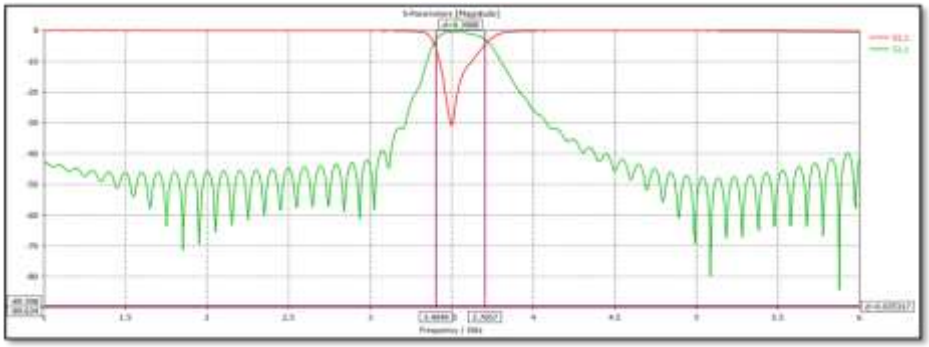


Figure 5. Simulated frequency response of the proposed 3.5 GHz Bandpass Filter

For the Butterworth-based coupled-line filter configuration, the simulated reflection coefficient (S_{11}) at the center frequency of 3.5 GHz is approximately -32 dB, indicating good impedance matching within the passband. The corresponding transmission coefficient (S_{21}) is measured as -0.73 dB at the center frequency, demonstrating low insertion loss across the operating band. In the stopband regions, the filter exhibits attenuation levels exceeding -40 dB, with deeper transmission nulls approaching -80 dB, confirming effective suppression of unwanted frequency components.

In addition to the magnitude responses, the group delay is evaluated as a critical parameter for assessing phase linearity within the passband. Group delay characterizes the rate of change of the transmission phase with respect to angular frequency and provides insight into signal distortion performance [21]. The simulated group delay response of the proposed filter is illustrated in Figure 6, demonstrating a relatively stable behavior across the operating band.

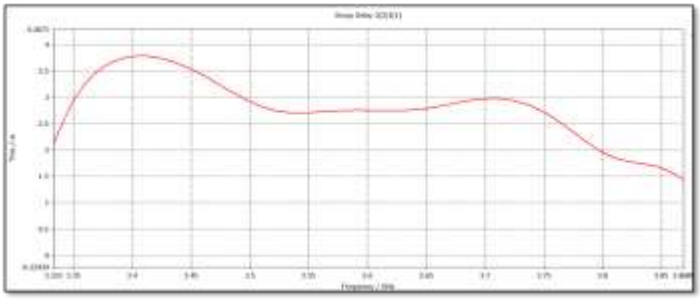


Figure 6. Group delay response of the proposed Bandpass Filter

The experimental characterization of the fabricated bandpass filter was carried out using a vector network analyzer under laboratory conditions. The measurement setup, including the fabricated filter prototype, coaxial cables, and SMA connectors, is shown in Figure 7. Care was taken to ensure proper calibration and stable electrical connections in order to minimize measurement uncertainties and external interference during the S-parameter measurements.

Figure 8 presents a comparative evaluation of the simulated and experimentally obtained S-parameter characteristics of the proposed filter. The measured return loss (S_{11}) and insertion loss (S_{21}) closely follow the trends predicted by numerical simulations throughout the frequency band of interest. The slight deviations observed between the two sets of results are mainly associated with manufacturing tolerances, connector-related effects, and inherent uncertainties in the dielectric properties of the FR-4 substrate. These findings verify that the fabricated prototype accurately reflects the intended bandpass response, thereby confirming the reliability of the adopted design methodology.



Figure 7. Measurement set-up

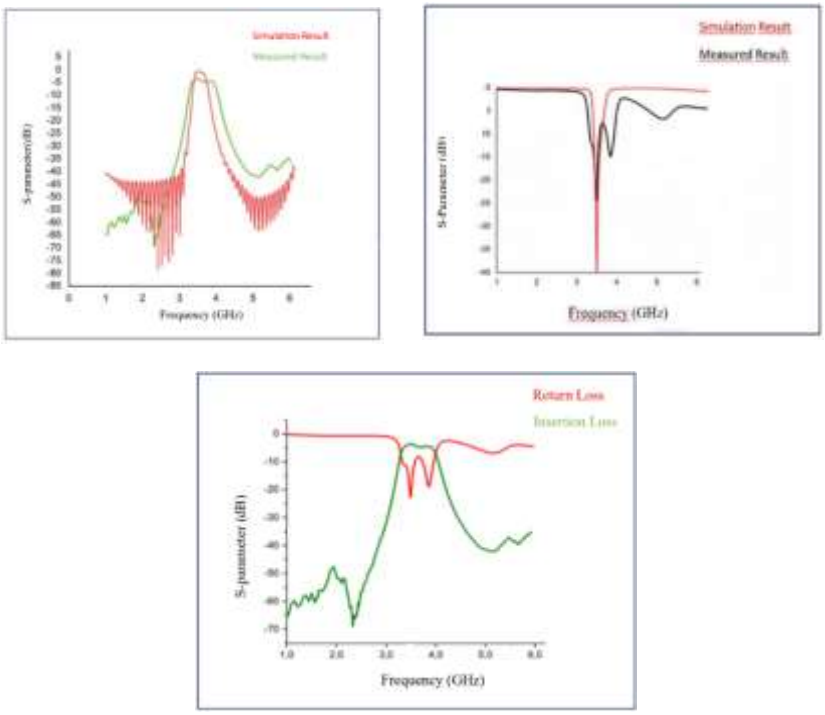


Figure 8. Simulated and measured S-parameter response of the proposed filter

The performance of the proposed bandpass filter is compared with several representative microstrip bandpass filters reported in the literature, as summarized in Table 3**.** The comparison includes key performance metrics such as return loss, insertion loss, operating bandwidth, physical dimensions, and substrate type. As shown in the table, the proposed filter achieves a competitive insertion loss while providing a wide operating bandwidth centered around the 3.5 GHz band. In addition, the overall physical size of the proposed design is comparable to or smaller than many existing implementations, despite being realized on a low-cost FR-4 substrate. These results demonstrate that the proposed filter offers a favorable trade-off between electrical performance, compactness, and fabrication cost when compared with previously reported bandpass filter designs. The performance of the proposed bandpass filter is compared with several representative microstrip bandpass filters reported in the literature [22]-[26]**,** as summarized in Table 3.

Table 3. Performance comparison of the proposed Bandpass Filter with previously reported designs

Return Loss	Insertion Loss	Bandwidth	Dimensions	Substrate	Reference
-25 dB	-0.1 dB	2.4 GHz-3.6 GHz	0.96 λ_o × 0.46 λ_o	AD600	[22]
-20 dB	-1.79 dB	2.96 GHz-3.140 GHz	0.57 λ_o × 0.56 λ_o	Duroid 5880	[23]
-12 dB	-0.49 dB	2.92 GHz-10.95 GHz	2.52 λ_o × 1.76 λ_o	AD260A	[24]
-17.3 dB	-2.2 dB	3.35 GHz - 4.5 GHz	0.79 λ_o × 0.39 λ_o	FR-4	[25]
-30 dB	-0.1 dB	2.5 GHz - 3.2 GHz	0.57 λ_o × 0.57 λ_o	F4BM	[26]
-31 dB	-0.75 dB	3.4 GHz -3.7 GHz	0.70 λ_o × 0.35 λ_o	FR-4	This study

4. CONCLUSION

In this study, a compact microstrip bandpass filter operating at a center frequency of 3.5 GHz has been presented for sub-6 GHz 5G applications. The filter is based on a fourth-order Butterworth response implemented using a coupled-line topology to achieve a flat passband characteristic and adequate frequency selectivity. Both simulated and measured results confirm an impedance bandwidth of approximately 300 MHz, covering the 3.35-3.65 GHz frequency range, with low insertion loss and satisfactory out-of-band attenuation. The experimental results show good agreement with the predicted performance, validating the proposed design approach and the adopted synthesis methodology. Owing to its compact physical dimensions, simple planar structure, and compatibility with low-cost substrate materials, the proposed filter is well suited for integration into RF front-end modules used in contemporary wireless communication systems. Future work may focus on extending the proposed topology toward reconfigurable or tunable bandpass filter implementations, enabling multiband operation and enhanced adaptability for emerging wireless standards beyond 5G.

Authors' Contributions

In this study, authors contributed equally to the study.

Competing Interests

The authors declare that they have no conflict of interest.

References

[1] Hsieh L.-H., Chang K., "Compact, low insertion-loss, sharp-rejection, and wide-band microstrip bandpass filters," IEEE Transactions on Microwave Theory and Techniques, Vol. 51, Iss: 4, (2003), pp.(1241-1246).
[2] Shin K.R., Arendell J., Eilert K., "Compact 5G n77 bandpass filter with through silicon via (TSV) IPD technology," in Proceedings of the 2019 IEEE 20th Wireless and Microwave Technology Conference (WAMICON), (2019), pp.(1-3).
[3] Lee K.C., Su H.T., Haldar M.K., "A review of centrally loaded multimode microstrip resonators for bandpass filter design," AEU-International Journal of Electronics and Communications, Vol. 69, Iss: 10, (2015), pp.(1533-1540).
[4] Shome P.P., Khan T., Koul S.K., Antar Y.M.M., "Two decades of UWB filter technology: Advances and emerging challenges in the design of UWB bandpass filters," IEEE Microwave Magazine, Vol. 22, Iss: 8, (2021), pp.(32-51).
[5] Li C., Ma Z.-H., Chen J.-X., Wang M.-N., Huang J.-M., "Design of a compact ultra-wideband microstrip bandpass filter," Electronics, Vol. 12, Iss: 7, (2023), pp.(1728).
[6] Dokmetas B., Arican G.O., Akcam N., Yazgan E., "A compact bandstop filter design using DMS-DGS technique for radar applications," ACES Journal, Vol. 36, Iss: 11, (2021), pp.(1460-1467).
[7] Dokmetas B., Arican G.O., "Design of dual-band SIW antenna for millimeter-wave communication," in 2023 31st Telecommunications Forum (TELFOR), Belgrade, Serbia, (2023), pp.(1-4).
[8] Dokmetas B., Belen M.A., "Microstrip antenna design for 2.4 GHz RF energy harvesting circuits with artificial neural networks," Journal of Artificial Intelligence and Data Science, Vol. 4, Iss: 1, (2024), pp.(33-38).
[9] Keskin S.E.B., Güller C., Uslu B., "Optimization of Monopole Consecutive Square-Shaped Patch Antenna with ANN for Wireless Communication Systems," El-Cezeri Journal of Science and Engineering, Vol. 10, Iss: 3, (2023), pp.(492-505).
[10] Kis G.E., Okan T., "Compact Power-Symbol Shaped Microstrip Antenna for Healthcare Monitoring Systems," El-Cezeri Journal of Science and Engineering, Vol. 9, Iss: 1, (2022), pp.(232-240).
[11] Guernine R., Sahed M., Kenane E., Djahli F., "A High-Efficient Single-Band Rectenna Design Using Dielectric Resonant Antenna for ISM Applications," El-Cezeri Journal of Science and Engineering, Vol. 13, Iss: 2, (2026), pp.(135-145).
[12] Cheng J., Alphones A., "Compact interdigital microstrip bandpass filter," Microwave and Optical Technology Letters, Vol. 52, Iss: 9, (2010), pp.(2128-2132).
[13] Chen C.-J., "A coupled-line coupling structure for the design of quasi-elliptic bandpass filters," IEEE Transactions on Microwave Theory and Techniques, Vol. 66, Iss: 4, (2018), pp.(1921-1925).
[14] Bisu A.A., "Design and simulation of a fourth-order high-frequency bandpass filter for radar communication systems," The Journal of the Nigerian Association of Mathematical Physics, Vol. 66, (2024), pp.(169-176).
[15] Yumnam K., Singh S., "A comprehensive analysis of bandpass filters for mmWave and sub-6 GHz 5G wireless communications," in Proceedings of the International Conference on Computational Electronics for Wireless Communications (ICCWC), (2023), pp.(331-342).
[16] Sheta A.F., Coupez J.P., Tanne G., Toutain S., Blot J.P., "Miniature microstrip stepped impedance resonator bandpass filters and diplexers for mobile communications," in 1996 IEEE MTT-S International Microwave Symposium Digest, Vol. 2, (1996), pp.(607-610).
[17] Ali M., Liu F., Watanabe A., Raj P.M., Sundaram V., Tentzeris M.M., Tummala R.R., "First demonstration of compact, ultra-thin low-pass and bandpass filters for 5G small-cell applications," IEEE Microwave and Wireless Components Letters, Vol. 28, Iss: 12, (2018), pp.(1110-1112).

[18] Michalkiewicz M.L., Mariano A.A., Dartora C.A., Castaldo F.C., "Bandpass filter using SIW technology in inductive window topology with low-cost FR-4 substrate," Journal of Microwaves, Optoelectronics and Electromagnetic Applications, Vol. 21, Iss: 1, (2022), pp.(83-101).
[19] Pozar D.M., Microwave engineering: theory and techniques, John Wiley & Sons, (2021).
[20] Zhu L., Sun S., Li R., Microwave bandpass filters for wideband communications, John Wiley & Sons, (2011).
[21] Martin P., Ness J., "Coupling bandwidth and reflected group delay characterization of microwave bandpass filters," Applied Microwave and Wireless, Vol. 11, (1999), pp.(86-96).
[22] Gruszczynski S., Staszek K., Wincza K., "Parallel-coupled bandpass filters with directly coupled input and output resonators," AEU-International Journal of Electronics and Communications, Vol. 172, (2023), pp.(154974).
[23] Darwis F., Rahayu E.A.B., Sutrisno S., Madiawati H., Taufiqqurrachman T., Setiawan A., Kurniawan E.D., Wijayanto Y.N., "Cross-coupled line bandpass filter based on modified parallel-coupled line structure," Jurnal Elektronika dan Telekomunikasi, Vol. 22, Iss: 1, (2022), pp.(8-13).
[24] Jamsai M., Angkawisittpan N., Nuan-On A., "Design of a compact ultra-wideband bandpass filter using inductively compensated parallel-coupled lines," Electronics, Vol. 10, Iss: 21, (2021), pp.(2575).
[25] Sani A.H., Jianwen C., Khan M.T., Yussif S.B., Nahar S., Ewald K.E., Ukwuoma C.C., "Design and simulation of a 3.9 GHz microstrip parallel-coupled line bandpass filter," in 2019 16th International Computer Conference on Wavelet Active Media Technology and Information Processing, (2019), pp.(429-433).
[26] La D.-S., Guan X., Wang M.-Y., Mi R.-Q., "Compact wideband bandpass filter based on coupled-line stub with high selectivity," AEU-International Journal of Electronics and Communications, Vol. 138, (2021), pp.(153872).